Available online at www.sciencedirect.com

ScienceDirect

International Journal of Solids and Structures 43 (2006) 6908–6920

INTERNATIONAL JOURNAL OF SOLIDS and STRUCTURES

www.elsevier.com/locate/ijsolstr

Steady-state creep analysis of pressurized pipe weldments by perturbation method

A.V. Shutov [a,*], H. Altenbach [b], K. Naumenko [b]

[a] *Lavrentyev Institute of Hydrodynamics of SB RAS, 630090 Novosibirsk, Russia*

[b] *Department of Engineering Sciences, Martin-Luther-University Halle-Wittenberg, D-06099 Halle, Germany*

Received 16 June 2005; received in revised form 6 December 2005
Available online 6 March 2006

Communicated by David A. Hills

Abstract

The stress analysis of pressurized circumferential pipe weldments under steady state creep is considered. The creep response of the material is governed by Norton's law. Numerical and analytical solutions are obtained by means of perturbation method, the unperturbed solution corresponds to the stress field in a homogeneous pipe. The correction terms are treated as stresses defined with the help of an auxiliary linear elastic problem. Exact expressions for jumps of hoop and radial stresses at the interface are obtained. The proposed technique essentially simplifies parametric analysis of multi-material components.

MSC: 74G10; 74D10; 74G70; 74S05

Keywords: Creep; Circumferential pipe weldments; Stress analysis; Parametric analysis; Perturbation method

1. Introduction

The welded pipelines subjected to high pressure and temperature are widely used in different branches of industry. Under such conditions, the creep and damage effects should be taken into account for accurate assurance of long-term reliability (Roche et al., 1992). Application of computational continuum creep damage mechanics (see, for example Altenbach et al., 2001; Hayhurst, 2001) coupled with increasing power of computers can accomplish this task. In recent years the finite element method has become the widely accepted tool for the structural analysis in the creep range (Hayhurst, 2001). A user defined creep material subroutine with appropriate constitutive and evolution equations can be developed and incorporated into the commercial finite element code to perform a numerical time step solution of creep and long term strength problems.

* Corresponding author.
E-mail address: shutov@ngs.ru (A.V. Shutov).

0020-7683/$ - see front matter © 2006 Elsevier Ltd. All rights reserved.
doi:10.1016/j.ijsolstr.2006.02.013

On the other hand, in addition to more and more sophisticated numerical analysis, simplified models of creep response are required. These models should provide a better intuitive insight into the problem and give a quantitative description of the solution.

The assessment of reliability of user-defined creep material subroutines and the choice of suitable numerical parameters like the element type, the mesh density, and time step control are complicated problems, particularly if studying creep of multi-material structures. Therefore, it is important to have reference solutions of benchmark problems. Such solutions should be obtained by use of alternative analytical or semi-analytical methods which do not require the spatial discretization techniques and allow for studying the behavior of stress and deformation gradients. The objective of this paper is to develop an alternative semi-analytical solutions to creep problems for multi-material pipe structures. Particularly we address the analysis of stress gradients in the local zones of material connections.

To obtain a semi-analytical solution we shall make the following simplifications. We assume the idealized material behavior having the secondary creep stage only. In this case the steady state solution of creep in the pipe exists, for which the stresses do not depend on time. We assume that the difference between the material properties of constituents is not great. Particularly the difference between the minimum creep rates for the same stress level should not exceed the factor of 2.

The lifetime of a welded pipe under creep conditions is less than that of homogeneous one. The effect of reliability reduction is of big interest, therefore large numbers of model problems were proposed. The most commonly used approach simulates weldment as a region with non-uniformly distributed material properties (Browne et al., 1981; Coleman et al., 1985; Hall and Hayhurst, 1991; Perrin and Hayhurst, 1999; Hayhurst et al., 2001; Hyde et al., 2003).

Within the framework of this approach it is often necessary to consider a number of parameter distribution cases. The amount of problems to be solved increases with the number of changing material parameters and parametric analysis becomes very complicated.

Drawing an analogy with some simple systems, for which an analytical solution is available (Hyde et al., 1996, 2000; Naumenko and Altenbach, 2005) is useful for understanding how the parameter change can affect the solution. However this is not enough for a proper estimation of stress distribution.

Two main types of constitutive equations are often used in weld modelling, namely, Norton's steady-state creep law and continuum damage mechanics equations for tertiary creep (Kachanov, 1986). Below only the constitutive equations of Norton's law are considered. Even by this assumption the structural response may be captured very well. Some special techniques are used to predict the failure life more precisely using steady-state solution (Leckie and Hayhurst, 1974; Nikitenko and Zaev, 1979; Hyde et al., 1998, 1999; Perrin et al., 2000). As shown in Browne et al. (1981), Coleman et al. (1985) for the particular pipe welds investigated, the steady-state analysis underestimates the failure time by about 20–40%, but predicts failure position quite well.

To simplify the parametric analysis, we study a family of boundary-value problems for multi-component pipe creep depending on a small parameter s. When $s = 0$, the problem is reduced to the case of homogeneous pipe creep. The corresponding solution $\boldsymbol{\sigma}(0)$ for the steady-state stress distribution is well known (Odqvist, 1974; Malinin, 1981; Hyde et al., 1996) and considered to be the basic solution. In order to get the common solution $\boldsymbol{\sigma}(s)$ from this basic one, correction terms should be added. The equations for the correction terms are formally obtained as perturbations of a boundary-value problem with respect to s. These equations formulate a problem of linear elasticity with respect to linear-elastic solid with anisotropic elastic properties.

The utility of used technique is guaranteed especially because the theory of linear elasticity is in a very satisfactory state of completion; every complicated case of parameter distribution can be treated in a routine manner as a combination of simple ones.

Correction terms are obtained numerically for some problems with the help of the Ritz method. In some cases the simplicity of geometry enables us to construct an approximate analytical solution. An exact analytical expression for stress jumps at the interface is obtained. Numerical solutions of the nonlinear problem are obtained with the help of ANSYS finite element code for comparison.

Throughout light-face letters we denote scalars, the bald-face letters stand for tensors. The notation $\vec{(\,)}$ is used in vector–matrix form of constitutive equations to designate vectors $\vec{\boldsymbol{\sigma}}$ and $\vec{\boldsymbol{\varepsilon}}$ of stress and strain components.

2. Problem formulation: two-material model of narrow gap weldment

In this section we consider a two-material model only. It will be shown later that the solution for some multi-material models can be reduced to this case.

The configuration analyzed is shown in Fig. 1. Assume that $(r,z,\theta) \in \Omega \times [0,2\pi)$, $(r,z,\theta) \in \Omega^- \times [0,2\pi)$, $(r,z,\theta) \in \Omega^+ \times [0,2\pi)$ describe the volume occupied by the solid, by the weld metal, and by the parent material, respectively. Here $\Omega^- = [r_i, r_o] \times [0,h)$, $\Omega^+ = [r_i, r_o] \times [h,H]$, $\Omega = \Omega^- \cup \Omega^+$. The basic equations of the problem are given below.

1. Equations of equilibrium

$$\nabla \cdot \boldsymbol{\sigma} = \mathbf{0}, \tag{1}$$

where $\boldsymbol{\sigma}$ is the stress tensor. In (1) the volumetric forces are ignored.

2. Strain–displacement relations

$$\boldsymbol{\varepsilon} = \frac{1}{2}\left(\nabla \mathbf{u} + \nabla \mathbf{u}^{\mathrm{T}}\right), \tag{2}$$

where $\boldsymbol{\varepsilon}$ is the linearized strain tensor and $\boldsymbol{u}$ is the displacement vector.

3. The governing equations can be summarized as Norton's creep law (see, for example, Odqvist, 1974)

$$\dot{\boldsymbol{\varepsilon}} = A\boldsymbol{s}(\sigma_{\mathrm{vM}})^{n-1}, \quad \boldsymbol{s} = \boldsymbol{\sigma} - \frac{1}{3}\mathrm{tr}(\boldsymbol{\sigma})\mathbf{I}, \quad \sigma_{\mathrm{vM}} = \sqrt{\frac{3}{2}\boldsymbol{s} : \boldsymbol{s}}, \tag{3}$$

where $\dot{(\ )}$ is the time derivative, $\boldsymbol{s}$ is the stress deviator, σ_{vM} is the von Mises equivalent stress, $\mathbf{I}$ is the second rank unit tensor, and A, n are material constants. Note that Norton's creep law is often written as $\dot{\boldsymbol{\varepsilon}} = \frac{3}{2}a\ \boldsymbol{s}(\sigma_{\mathrm{vM}})^{n-1}$. It means $A = \frac{3}{2}a$ in our notation.

If we take into account that the problem is axisymmetric, we have in cylindrical coordinates the following equilibrium equations

$$\frac{\partial \sigma_r}{\partial r} + \frac{1}{r}(\sigma_r - \sigma_\theta) + \frac{\partial \sigma_{rz}}{\partial z} = 0, \quad \frac{\partial \sigma_{rz}}{\partial r} + \frac{1}{r}\sigma_{rz} + \frac{\partial \sigma_z}{\partial z} = 0, \tag{4}$$

strain–displacement relations

$$\varepsilon_r = \frac{\partial u_r}{\partial r}, \quad \varepsilon_\theta = \frac{u_r}{r}, \quad \varepsilon_z = \frac{\partial u_z}{\partial z}, \quad \varepsilon_{rz} = \frac{1}{2}\left(\frac{\partial u_r}{\partial z} + \frac{\partial u_z}{\partial r}\right), \tag{5}$$

and boundary conditions

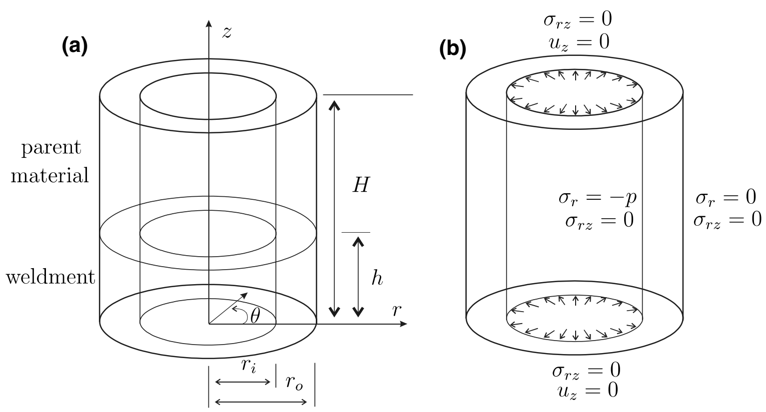

Fig. 1. System configuration (a) and boundary conditions (b).

$$\begin{aligned} &\sigma_r = -p, \ \sigma_{rz} = 0 \ \text{ at } r = r_{\text{i}}; \quad \sigma_r = \sigma_{rz} = 0 \ \text{ at } r = r_{\text{o}}; \\ &\sigma_{rz} = 0, \ u_z = 0 \quad \text{at } z = 0, \ z = H. \end{aligned} \tag{6}$$

Finally we define the distribution of the parameter $A(r,z)$ in Norton's creep law (3) as a piecewise constant function in Ω

$$A = A^+ \ \text{ in } \Omega^+, \quad A = A^- \ \text{ in } \Omega^-. \tag{7}$$

The stress field $\boldsymbol{\sigma}$, defined by (1)–(7), does not change if instead of $A(r,z)$ we use $\lambda A(r,z)$, where λ is any non-zero constant. Consequently, without loss of generality it can be assumed that[1]

$$A = A^+ = 1 \ \text{ in } \Omega^+, \quad A = A^- = 1 - s \ \text{ in } \Omega^-. \tag{8}$$

If we eliminate displacements from the strain–displacement relations (5), we obtain compatibility equations

$$C_1(\boldsymbol{\varepsilon}) = C_2(\boldsymbol{\varepsilon}) = 0, \tag{9}$$

$$C_1(\boldsymbol{\varepsilon}) = r\left(\varepsilon_r - \frac{\partial(r\varepsilon_\theta)}{\partial r}\right), \quad C_2(\boldsymbol{\varepsilon}) = r\frac{\partial^2\varepsilon_\theta}{\partial z^2} + \frac{\partial\varepsilon_z}{\partial r} - 2\frac{\partial\varepsilon_{rz}}{\partial z}. \tag{10}$$

We consider the weak form of compatibility equations expressed by the equation of complementary virtual power principle (Washizu, 1982)

$$\begin{aligned} &L(\boldsymbol{\sigma}, s)\langle\delta\boldsymbol{\sigma}\rangle = 0, \quad \forall\delta\boldsymbol{\sigma}, \\ &L(\boldsymbol{\sigma}, s)\langle\delta\boldsymbol{\sigma}\rangle \equiv \int_\Omega \dot{\boldsymbol{\varepsilon}}(\boldsymbol{\sigma}, s) : \delta\boldsymbol{\sigma}\,\mathrm{d}\Omega. \end{aligned} \tag{11}$$

Here we use the brackets $\langle\cdot\rangle$ to enclose the argument of a linear operator; $\dot{\boldsymbol{\varepsilon}}(\boldsymbol{\sigma}, s)$ is the strain rate defined by (3) and (8); $\mathrm{d}\Omega = r\,\mathrm{d}r\,\mathrm{d}z$; $\delta\boldsymbol{\sigma}$ is a virtual stress field that satisfy the equations of equilibrium (4) and homogeneous boundary conditions

$$\sigma_r = \sigma_{rz} = 0 \ \text{ at } r = r_{\text{i}}, \ r = r_{\text{o}}; \quad \sigma_{rz} = 0 \ \text{ at } z = 0, \ z = H. \tag{12}$$

In what follows we search function $\boldsymbol{\sigma}(s)$, such that

$$L(\boldsymbol{\sigma}(s), s)\langle\delta\boldsymbol{\sigma}\rangle = 0, \quad \forall\delta\boldsymbol{\sigma}. \tag{13}$$

3. Perturbation method

3.1. Unperturbed solution: creep response of a homogeneous pipe

Now suppose that $A^+ = A^-$, i.e. $s = 0$. The problem (11) is reduced to a one-dimensional, and the solution $\boldsymbol{\sigma}^0$ of this problem is well known (Odqvist, 1974; Malinin, 1981; Hyde et al., 1996)

$$\begin{aligned} &\sigma^0_r = a + a_r r^{-2/n}, \quad \sigma^0_\theta = a + a_\theta r^{-2/n}, \quad \sigma^0_z = a + a_z r^{-2/n}, \quad \sigma^0_{rz} = 0, \\ &a = p\frac{r_{\text{i}}^{2/n}}{r_{\text{o}}^{2/n} - r_{\text{i}}^{2/n}}, \quad a_r = -p\frac{r_{\text{i}}^{2/n} r_{\text{o}}^{2/n}}{r_{\text{o}}^{2/n} - r_{\text{i}}^{2/n}}, \quad a_\theta = \frac{n-2}{n}a_r, \quad a_z = \frac{n-1}{n}a_r. \end{aligned} \tag{14}$$

3.2. First perturbation

Let s be a small parameter. Assume that[2]

$$\boldsymbol{\sigma}(s) = \boldsymbol{\sigma}^0 + s\boldsymbol{\sigma}^1 + \mathrm{o}(s). \tag{15}$$

---

[1] Here s is not necessary a small parameter. In practice, A^+ and A^- might differ essentially.

[2] The justification of perturbation method could be performed by means of Implicit Function Theorem (Antman, 1995). Precise conditions justifying perturbation method should be formulated in an appropriate function space.

Here $\boldsymbol{\sigma}^1 = \frac{d\boldsymbol{\sigma}(s)}{ds}\Big|_{s=0}$ is the unknown derivative which must satisfy the equations of equilibrium (4) and the homogeneous boundary conditions (12); $o(s)$ is the little-o Landau symbol. From (8) it follows that:

$$L(\boldsymbol{\sigma}, s)\langle \delta\boldsymbol{\sigma}\rangle = \left(L^0(\boldsymbol{\sigma}) + sL^1(\boldsymbol{\sigma})\right)\langle \delta\boldsymbol{\sigma}\rangle \tag{16}$$

with $L^0(\boldsymbol{\sigma}) \equiv L(\boldsymbol{\sigma}, 0)$, $L^1(\boldsymbol{\sigma}) \equiv \frac{\partial L(\boldsymbol{\sigma}, s)}{\partial s}$. Substituting (15) and (16) in (13), we get

$$\left(L^0(\boldsymbol{\sigma}^0) + s\frac{dL^0}{d\boldsymbol{\sigma}}\Big|_{\boldsymbol{\sigma}=\boldsymbol{\sigma}^0}\langle \boldsymbol{\sigma}^1\rangle + sL^1(\boldsymbol{\sigma}^0) + o(s)\right)\langle \delta\boldsymbol{\sigma}\rangle = 0.$$

Since $L^0(\boldsymbol{\sigma}^0)\langle \delta\boldsymbol{\sigma}\rangle = 0$ and $\frac{o(s)}{s}\langle \delta\boldsymbol{\sigma}\rangle \to 0$ as $s \to 0$, we have an equation for $\boldsymbol{\sigma}^1$

$$\frac{dL^0}{d\boldsymbol{\sigma}}\Big|_{\boldsymbol{\sigma}=\boldsymbol{\sigma}^0}\langle \boldsymbol{\sigma}^1\rangle\langle \delta\boldsymbol{\sigma}\rangle = -L^1(\boldsymbol{\sigma}^0)\langle \delta\boldsymbol{\sigma}\rangle, \quad \forall \delta\boldsymbol{\sigma}. \tag{17}$$

We will analyze more closely the linear operator $\frac{dL^0}{d\boldsymbol{\sigma}}\Big|_{\boldsymbol{\sigma}=\boldsymbol{\sigma}^0}\langle\cdot\rangle$ in the next section.

4. Auxiliary problem

4.1. Linear elastic material

In the previous section it was shown that the correction term $\boldsymbol{\sigma}^1$ can be found from the linear Eq. (17). It is clear that

$$\frac{dL^0}{d\boldsymbol{\sigma}}\Big|_{\boldsymbol{\sigma}=\boldsymbol{\sigma}^0}\langle \boldsymbol{\sigma}^1\rangle\langle \delta\boldsymbol{\sigma}\rangle = \int_\Omega \frac{\partial \dot{\boldsymbol{\varepsilon}}}{\partial \boldsymbol{\sigma}}(\boldsymbol{\sigma}^0, 0)\langle \sigma^1\rangle : \delta\boldsymbol{\sigma}\, d\Omega, \tag{18}$$

where

$$\dot{\boldsymbol{\varepsilon}}(\boldsymbol{\sigma}, 0) = \boldsymbol{s}(\boldsymbol{\sigma})(\sigma_{\mathrm{vM}}(\boldsymbol{\sigma}))^{n-1}. \tag{19}$$

Let us introduce a vector notation $\vec{(\,)}$ as

$$\vec{\boldsymbol{\sigma}} = (\sigma_r, \sigma_\theta, \sigma_z, \sigma_{rz})^{\mathrm{T}}, \quad \vec{\boldsymbol{\varepsilon}} = (\varepsilon_r, \varepsilon_\theta, \varepsilon_z, 2\varepsilon_{rz})^{\mathrm{T}}. \tag{20}$$

Substituting (20) in (18) and differentiating (19) we obtain

$$\frac{dL^0}{d\boldsymbol{\sigma}}\Big|_{\boldsymbol{\sigma}=\boldsymbol{\sigma}^0}\langle \boldsymbol{\sigma}^1\rangle\langle \delta\boldsymbol{\sigma}\rangle = \int_\Omega (\vec{\boldsymbol{\sigma}^1})^{\mathrm{T}}\mathbf{C}\delta\vec{\boldsymbol{\sigma}}\, d\Omega. \tag{21}$$

Here we have introduced the compliance matrix as follows:

$$\mathbf{C} = \frac{\partial \vec{\boldsymbol{\varepsilon}}}{\partial \vec{\boldsymbol{\sigma}}}(\vec{\boldsymbol{\sigma}^0}) = \left(\sqrt{3}\frac{|a_r|}{n}r^{-2/n}\right)^{n-2}\begin{bmatrix} 2/3 + (n-1)/2 & -1/3 - (n-1)/2 & -1/3 & 0 \\ & 2/3 + (n-1)/2 & -1/3 & 0 \\ \text{sym} & & -1/3 & 0 \\ & & & 2 \end{bmatrix}. \tag{22}$$

Thus, the left-hand side of (17) can be treated as an internal complementary virtual work with respect to linear elastic solid with constitutive law

$$(\varepsilon_r, \varepsilon_\theta, \varepsilon_z, 2\varepsilon_{rz})^{\mathrm{T}} = \mathbf{C}(\sigma_r, \sigma_\theta, \sigma_z, \sigma_{rz})^{\mathrm{T}}. \tag{23}$$

The eigenvalues of the compliance operator $\boldsymbol{C}$ are

$$(\lambda_1, \lambda_2, \lambda_3, \lambda_4) = \left(\sqrt{3}\frac{|a_r|}{n}r^{-2/n}\right)^{n-2}(0, 2, 2, n). \tag{24}$$

The problem of steady-state creep is reduced to the elasticity problem for orthotropic, incompressible, and inhomogeneous solid (23).

4.2. Displacement jump

We now seek to convert the right-hand side of (17) into a surface integral through Gauss theorem. It can be proved that

$$-L^1(\boldsymbol{\sigma}^0)\langle\delta\boldsymbol{\sigma}\rangle = \int_{\Omega^-} \dot{\boldsymbol{\varepsilon}}(\boldsymbol{\sigma}^0, 0) : \delta\boldsymbol{\sigma}\,\mathrm{d}\Omega = -\int_{\{z=h\}} 3^{\frac{n-1}{2}} a_r |a_r|^{n-1} \frac{1}{rn^n} \delta\sigma_{rz} r\,\mathrm{d}r. \tag{25}$$

Let us show that (25) prescribes a jump of displacements at the interface $\{z = h\}$ (see Fig. 2). Consider the principle of virtual complementary work for linear elastic solids Ω^- and Ω^+. One gets

$$\int_{\Omega^-} (\vec{\boldsymbol{\sigma}^-})^{\mathrm{T}} \mathbf{C} \delta\vec{\boldsymbol{\sigma}}\,\mathrm{d}\Omega = \int_{\{z=h\}} (u_r^- \delta\sigma_{rz} + u_z^- \delta\sigma_z) r\,\mathrm{d}r, \tag{26}$$

$$\delta\sigma_r = \delta\sigma_{rz} = 0 \ \text{ at } r = r_{\mathrm{i}},\ r = r_{\mathrm{o}}; \quad \delta\sigma_{rz} = 0 \ \text{ at } z = 0. \tag{27}$$

$$\int_{\Omega^+} (\vec{\boldsymbol{\sigma}^+})^{\mathrm{T}} \mathbf{C}\ \delta\vec{\boldsymbol{\sigma}}\,\mathrm{d}\Omega = -\int_{\{z=h\}} (u_r^+ \delta\sigma_{rz} + u_z^+ \delta\sigma_z) r\,\mathrm{d}r, \tag{28}$$

$$\delta\sigma_r = \delta\sigma_{rz} = 0 \ \text{ at } r = r_{\mathrm{i}},\ r = r_{\mathrm{o}}; \quad \delta\sigma_{rz} = 0 \ \text{ at } z = H. \tag{29}$$

Suppose

$$\sigma_{rz}^+ - \sigma_{rz}^- = 0, \quad \sigma_z^+ - \sigma_z^- = 0 \ \text{ at } z = h; \tag{30}$$

$$u_z^+ - u_z^- = 0, \quad u_r^+ - u_r^- = 3^{\frac{n-1}{2}} a_r |a_r|^{n-1} \frac{1}{rn^n} \ \text{ at } z = h; \tag{31}$$

then it can be shown that the solution $\boldsymbol{\sigma}^1$ of (17) has the form

$$\boldsymbol{\sigma}^1 = \begin{cases} \boldsymbol{\sigma}^+ & \text{in } \Omega^+, \\ \boldsymbol{\sigma}^- & \text{in } \Omega^-. \end{cases} \tag{32}$$

4.3. Stress jump

We define a notation for jumps of field variables at the interface $\{z = h\}$

$$[v] = v^+ - v^-.$$

Substituting (31) for u_r in (5), we get

$$[\varepsilon_r] = -c/r^2, \quad [\varepsilon_\theta] = c/r^2, \quad c = 3^{\frac{n-1}{2}} a_r |a_r|^{n-1} \frac{1}{n^n}.$$

If we combine this with (22), (23), and (30), we obtain

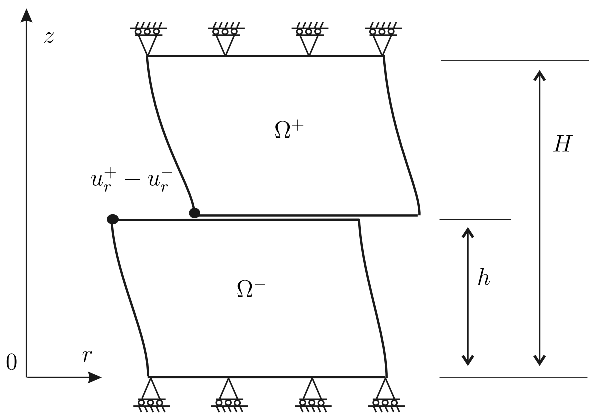

Fig. 2. Displacement jump.

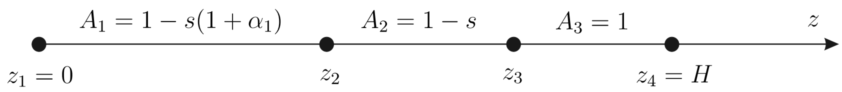

Fig. 3. Distribution of A in m-material structure ($m = 3$).

$$[\sigma_r^1] = -\frac{\sqrt{3}a_r|a_r|}{n^3}r^{-4/n}, \quad [\sigma_\theta^1] = \frac{\sqrt{3}a_r|a_r|}{n^3}r^{-4/n}. \tag{33}$$

4.4. Case of multi-material structure

In this subsection we consider m-material structure ($m \geqslant 2$)

$$\Omega = \Omega_1 \cup \Omega_2 \cup \dots \cup \Omega_m,$$
$$\Omega_j = [r_{\rm i}, r_{\rm o}] \times [z_j, z_{j+1}], \quad z_1 = 0, \quad z_{m+1} = H,$$
$$A = A_j \text{ in } \Omega_j, \ j = 1, \dots, m; \quad A_m = 1, \quad A_{m-1} \neq A_m.$$

There exist unique s and α_j, $j = 1, \dots, m-1$ such that (Fig. 3)

$$A(z) = 1 - s\sum_{j=1}^{m-1} \alpha_j H(z_{j+1} - z), \quad \alpha_{m-1} = 1. \tag{34}$$

Here $H(z)$ is the Heaviside function.

If we use the small parameter method to solve this problem, then we get an approximation in the form (15); $\boldsymbol{\sigma}^0$ is given by (14) and $\boldsymbol{\sigma}^1$ is obtained from (17). Since (34) is valid, it follows that the right-hand side of (17) has the form

$$-L^1(\boldsymbol{\sigma}^0)\langle\delta\boldsymbol{\sigma}\rangle = \sum_{j=1}^{m-1} \alpha_j \int_{\{z=z_j\}} \frac{-c}{r}\delta\sigma_{rz} r\,\mathrm{d}r.$$

Owing to the fact that (17) is linear, the perturbation $\boldsymbol{\sigma}^1$ is a linear combination of $m-1$ solutions of type (32).

5. Solution techniques

5.1. Approximate analytical solution

In this section we construct an analytical solution for the first perturbation term $\boldsymbol{\sigma}^1$. Consider a pair of stress functions (φ, ψ), such that condition (4) is satisfied

$$\sigma_r = \varphi, \quad \sigma_\theta = \frac{\partial(r\varphi)}{\partial r} + \frac{\partial^2\psi}{\partial z^2}, \quad \sigma_z = -\frac{1}{r}\frac{\partial\psi}{\partial r}, \quad \sigma_{rz} = \frac{1}{r}\frac{\partial\psi}{\partial z}. \tag{35}$$

These functions were constructed from compatibility equations (9) and (10) using the standard technique (Washizu, 1982). This choice of stress functions simplifies the application of variational methods.

We use the Kantorovich method (see, for example, Kantorovich and Krylov, 1958) to reduce the 2-D variational problem to 1-D variational problem. Suppose that for (φ, ψ), that define the solution $\boldsymbol{\sigma}^1$ of (17), the following static hypothesis is valid

$$\varphi(r,z) = \varphi_1(r)\varphi_2(z), \quad \psi(r,z) = \psi_1(r)\psi_2(z), \tag{36}$$

where $\varphi_1(r)$, $\psi_1(r)$ are given Kantorovich trial functions, such that

$$\varphi_1(r_{\rm i}) = \varphi_1(r_{\rm o}) = \psi_1(r_{\rm i}) = \psi_1(r_{\rm o}) = 0.$$

We use the Kantorovich method to obtain a system of differential equations and boundary conditions for $\varphi_2(z)$, $\psi_2(z)$. This method gives a projection of $\boldsymbol{\sigma}^1$ on the subspace, defined by (36). It is more convenient to solve (17) in the form (26)–(32). For the sake of brevity we describe only the application of the Kantorovich method for Eq. (26). For Eq. (28) this procedure can be arranged in a similar manner.

Since $\varphi_1(r)$ and $\psi_1(r)$ are fixed, the variation of (36) gives

$$\delta\varphi = \varphi_1(r)\delta\varphi_2(z), \quad \delta\psi = \psi_1(r)\delta\psi_2(z). \tag{37}$$

Let us rewrite (26) and (27) in terms of φ_2, ψ_2

$$\int_{\Omega^-} (\vec{\boldsymbol{\sigma}}(\varphi_2,\psi_2))^{\mathrm{T}}\mathbf{C}\vec{\boldsymbol{\sigma}}(\delta\varphi_2,\delta\psi_2)\,\mathrm{d}\Omega = \int_{r_{\mathrm{i}}}^{r_{\mathrm{o}}} \left(u_r^- \frac{\psi_1(r)}{r}\frac{\mathrm{d}\delta\psi_2}{\mathrm{d}z}(h) - u_z^- \frac{\delta\psi_2(h)}{r}\frac{\mathrm{d}\psi_1(r)}{\mathrm{d}r}\right) r\,\mathrm{d}r,$$
$$\frac{\mathrm{d}\psi_2}{\mathrm{d}z}(0) = 0, \quad \frac{\mathrm{d}\delta\psi_2}{\mathrm{d}z}(0) = 0.$$

Here $\vec{\boldsymbol{\sigma}}(\varphi_2,\psi_2)$ and $\vec{\boldsymbol{\sigma}}(\delta\varphi_2,\delta\psi_2)$ are defined by (20), (36), and (37). Using Gauss theorem and the fundamental lemma of the calculus of variation (Washizu, 1982) we obtain compatibility equations and boundary conditions

$$\int_{r_{\mathrm{i}}}^{r_{\mathrm{o}}} \varphi_1(r) C_1(\vec{\boldsymbol{\varepsilon}}(\varphi_2,\psi_2))\,\mathrm{d}r = 0, \quad \int_{r_{\mathrm{i}}}^{r_{\mathrm{o}}} \psi_1(r) C_2(\vec{\boldsymbol{\varepsilon}}(\varphi_2,\psi_2))\,\mathrm{d}r = 0, \tag{38}$$

$$\int_{\{z=0\}} \left(2\varepsilon_{rz} - \frac{\partial(r\varepsilon_\theta)}{\partial z}\right)\psi_1(r)\,\mathrm{d}r = 0, \int_{\{z=h\}} \left(2\varepsilon_{rz} - \frac{\partial(r\varepsilon_\theta)}{\partial z} - \frac{\mathrm{d}u_z^-}{\mathrm{d}r}\right)\psi_1(r)\,\mathrm{d}r = 0, \tag{39}$$

$$\int_{\{z=h\}} \left(\varepsilon_\theta - \frac{u_r^-}{r}\right)\psi_1(r)\,\mathrm{d}r = 0. \tag{40}$$

Here $\vec{\boldsymbol{\varepsilon}} = \mathbf{C}\vec{\boldsymbol{\sigma}}$ and $C_1(\vec{\boldsymbol{\varepsilon}})$, $C_2(\vec{\boldsymbol{\varepsilon}})$ are defined by (10), (20). After integration, system (38) has the form

$$a_1\varphi_2 + a_2\psi_2 + a_3\frac{\mathrm{d}^2\psi_2}{\mathrm{d}z^2} = 0, \quad b_1\varphi_2 + b_2\frac{\mathrm{d}^2\varphi_2}{\mathrm{d}z^2} + b_3\psi_2 + b_4\frac{\mathrm{d}^2\psi_2}{\mathrm{d}z^2} + b_5\frac{\mathrm{d}^4\psi_2}{\mathrm{d}z^4} = 0. \tag{41}$$

Elimination of φ_2 from (41) gives

$$k_1\psi_2 + k_2\frac{\mathrm{d}^2\psi_2}{\mathrm{d}z^2} + k_3\frac{\mathrm{d}^4\psi_2}{\mathrm{d}z^4} = 0. \tag{42}$$

After integration in (39) and (40), we obtain

$$\left(e_1\frac{\mathrm{d}\psi_2}{\mathrm{d}z} + e_2\frac{\mathrm{d}^2\psi_2}{\mathrm{d}z^2} + e_3\frac{\mathrm{d}^3\psi_2}{\mathrm{d}z^3}\right)(0) = 0,$$
$$\left(e_1\frac{\mathrm{d}\psi_2}{\mathrm{d}z} + e_2\frac{\mathrm{d}^2\psi_2}{\mathrm{d}z^2} + e_3\frac{\mathrm{d}^3\psi_2}{\mathrm{d}z^3}\right)(h) = \int_{\{z=h\}} \frac{\mathrm{d}u_z^-}{\mathrm{d}r}\psi_1(r)\,\mathrm{d}r,$$
$$\left(g_1\psi_2 + g_2\frac{\mathrm{d}^2\psi_2}{\mathrm{d}z^2}\right)(h) = \int_{\{z=h\}} \frac{u_r^-}{r}\psi_1(r)\,\mathrm{d}r.$$

Dealing with (28), (29) in a similar fashion we obtain compatibility equations and boundary conditions for $\psi_2(z)$ in (h,H). Finally, taking into account (30) and (31), we have eight boundary conditions

$$\frac{\mathrm{d}\psi_2}{\mathrm{d}z}(0) = 0, \quad \frac{\mathrm{d}\psi_2}{\mathrm{d}z}(H) = 0,$$
$$[\psi_2] = 0, \quad \left[\frac{\mathrm{d}\psi_2}{\mathrm{d}z}\right] = 0,$$
$$\left(e_1\frac{\mathrm{d}\psi_2}{\mathrm{d}z} + e_2\frac{\mathrm{d}^2\psi_2}{\mathrm{d}z^2} + e_3\frac{\mathrm{d}^3\psi_2}{\mathrm{d}z^3}\right)(0) = 0,$$
$$\left(e_1\frac{\mathrm{d}\psi_2}{\mathrm{d}z} + e_2\frac{\mathrm{d}^2\psi_2}{\mathrm{d}z^2} + e_3\frac{\mathrm{d}^3\psi_2}{\mathrm{d}z^3}\right)(H) = 0,$$
$$\left[e_1\frac{\mathrm{d}\psi_2}{\mathrm{d}z} + e_2\frac{\mathrm{d}^2\psi_2}{\mathrm{d}z^2} + e_3\frac{\mathrm{d}^3\psi_2}{\mathrm{d}z^3}\right] = 0,$$
$$\left[g_1\psi_2 + g_2\frac{\mathrm{d}^2\psi_2}{\mathrm{d}z^2}\right] = \int_{r_{\mathrm{i}}}^{r_{\mathrm{o}}} \frac{c}{r^2}\psi_1(r)\,\mathrm{d}r.$$

Solution $\psi_2(z)$ is uniquely defined by these equations combined with two ordinary differential equations (ODE) (42) of fourth order (one equation in $(0,h)$ and another in (h,H)).

5.2. Numerical solution technique

In this section we solve problem (17) numerically with the help of the Ritz method. Let $\boldsymbol{\sigma}_i$, $i=1,2,\ldots,N$ be a system of stresses, satisfying (4) and (12). Suppose

$$\boldsymbol{\sigma}^1 = \sum_{i=1}^{N} c_i \boldsymbol{\sigma}_i.$$

Then the unknown constants c_{i} are defined from a system of N linear algebraic equations

$$\left.\frac{\mathrm{d}L^0}{\mathrm{d}\boldsymbol{\sigma}}\right|_{\boldsymbol{\sigma}=\boldsymbol{\sigma}^0} \langle \boldsymbol{\sigma}^1\rangle\langle \boldsymbol{\sigma}_i\rangle = -L^1(\boldsymbol{\sigma}^0)\langle \boldsymbol{\sigma}_i\rangle, \quad i=1,\ldots,N.$$

We use the system $\boldsymbol{\sigma}_i$, $i=1,2,\ldots$, produced by means of (35). The complete system of φ, ψ is given by combinations of trigonometric functions

$$\varphi = \sin\left(i\frac{r-r_{\mathrm{i}}}{r_{\mathrm{o}}-r_{\mathrm{i}}}\pi\right)\cos\left(j\frac{z\pi}{H}\right), \quad i=1,2,\ldots,N_r,\ j=0,1,\ldots,N_z, \tag{43}$$

$$\varphi = \sin\left(i\frac{r-r_{\mathrm{i}}}{r_{\mathrm{o}}-r_{\mathrm{i}}}\pi\right)\cos\left(\frac{z\pi}{2H}\right), \quad i=1,2,\ldots,N_r, \tag{44}$$

$$\varphi = \sin\left(i\frac{r-r_{\mathrm{i}}}{r_{\mathrm{o}}-r_{\mathrm{i}}}\pi\right)\sin\left(\frac{z\pi}{2H}\right), \quad i=1,2,\ldots,N_r, \tag{45}$$

$$\psi = \sin\left(n\frac{r-r_{\mathrm{i}}}{r_{\mathrm{o}}-r_{\mathrm{i}}}\pi\right)\cos\left(k\frac{z\pi}{H}\right), \quad n=1,2,\ldots,N_r,\ k=0,1,\ldots,N_z. \tag{46}$$

In order to approximate the stress-jump (33) at the interface $\{z=h\}$ it could be useful to consider additionally discontinuous functions

$$\varphi = \sin\left(i\frac{r-r_{\mathrm{i}}}{r_{\mathrm{o}}-r_{\mathrm{i}}}\pi\right)H(z), \quad i=1,2,\ldots,N_r, \tag{47}$$

$$\psi = \sin\left(n\frac{r-r_{\mathrm{i}}}{r_{\mathrm{o}}-r_{\mathrm{i}}}\pi\right)\begin{cases}\dfrac{z^2}{2h}, & z<h\\[2mm] \dfrac{-z^2}{2(H-h)}+\dfrac{zH}{H-h}+\dfrac{-hH}{2(H-h)}, & z\geqslant h\end{cases}, \quad n=1,2,\ldots,N_r. \tag{48}$$

Here $H(z)$ is the Heaviside function.

If we put $N_r=1$, $N_z\to\infty$, then the solution tends to the approximate analytical solution from the previous section.

6. Results of calculations

The specimen dimensions, applied loads, and material constants are given by $H=8$, $h=0.5$, $r_{\mathrm{i}}=1$, $r_{\mathrm{o}}=2$, $p=1$, $n=3$.

6.1. Solution of the linear auxiliary problem

First we compare the approximate analytical solution of (17) (Section 5.1) with the numerical solution which was obtained using the Ritz method (Section 5.2).

We used $\varphi_1(r)=\psi_1(r)=\sin\left(\frac{r-r_{\mathrm{i}}}{r_{\mathrm{o}}-r_{\mathrm{i}}}\pi\right)$ in (36) to construct the analytical solution. Values of constants a_{i}, b_{i}, k_{i}, e_{i}, g_{i} are given in Appendix A. The numerical solution by the Ritz method is performed with $N_r=N_z=25$ in (43)–(48).

We use $r = 1, 5$ to illustrate in Fig. 4 the distribution of stress components along the z axis. Along $r = 1, 5$ the σ_z stress is negligibly small for both solutions, therefore we do not plot this component.

Hypothesis (36) imposes essential restrictions on the class of solutions, nevertheless the value of shear stress σ_{rz} is captured very well. The error for the hoop stress σ_θ and the radial σ_r stress is significant in the vicinity of the interface $\{z = h\}$.

The approximate analytical solution gives only a smooth part of the stress field. This solution can be more useful in case of smooth changing material properties.

6.2. Solution of the nonlinear problem

We investigate the error of the perturbation method $o(s) = \boldsymbol{\sigma}(s) - (\boldsymbol{\sigma}^0 + s\boldsymbol{\sigma}^1)$.

Numerical solutions $\boldsymbol{\sigma}(s)$ of the system (1)–(8) are obtained with the help of ANSYS finite element code for a set of s. The geometry of the half of the pipe was represented by 3200 axisymmetric PLANE183 finite elements (Fig. 5). We used a uniform mesh with 160 elements along the axis direction z and 20 elements along the radial direction r. This type of element can model creep behavior but the Norton's constitutive law is available only as a secondary creep equation. That is, the total strain is a sum of elastic strain and creep strain

$$\boldsymbol{\varepsilon} = \boldsymbol{\varepsilon}^{el} + \boldsymbol{\varepsilon}^{cr}.$$

If the applied load remains the same with time t, then we have

$$\boldsymbol{\varepsilon} \approx \boldsymbol{\varepsilon}^{cr} \quad \text{as } t \to \infty,$$

and we obtain the steady-creep solution as $t \to \infty$. In calculations we used $E = 100$ for Young's modulus and $\nu = 0.3$ for Poisson's ratio to simulate the elastic material. We consider the solution to be close enough to the asymptotic solution at the moment $T = 100$ of time t.

The solution $\boldsymbol{\sigma}^1$ of the auxiliary problem is given by the Ritz method (see Section 5.2). Here we used series (43)–(48) with $N_r = N_z = 25$.

The leading term in the asymptotic series is a good approximation even if the "small" parameter s equals 0.5 (Fig. 6). With subsequent increase of s the error grows dramatically.

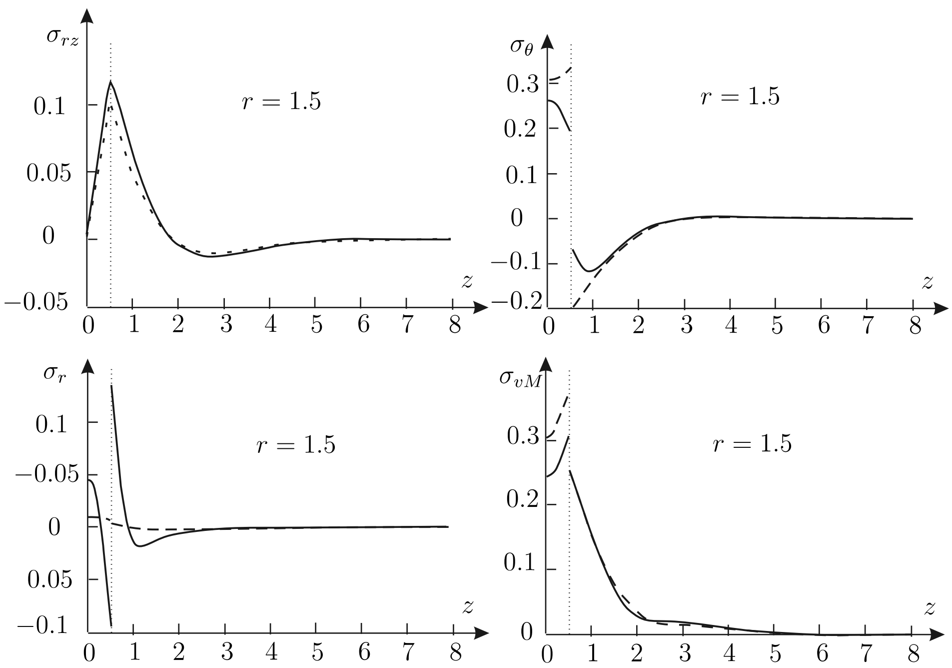

Fig. 4. Comparison of the approximate analytical solution (dashed line) with numerical solution, obtained by the Ritz method (solid line).

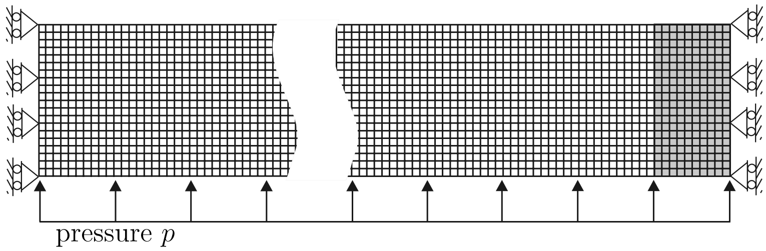

Fig. 5. FE mesh and boundary conditions.

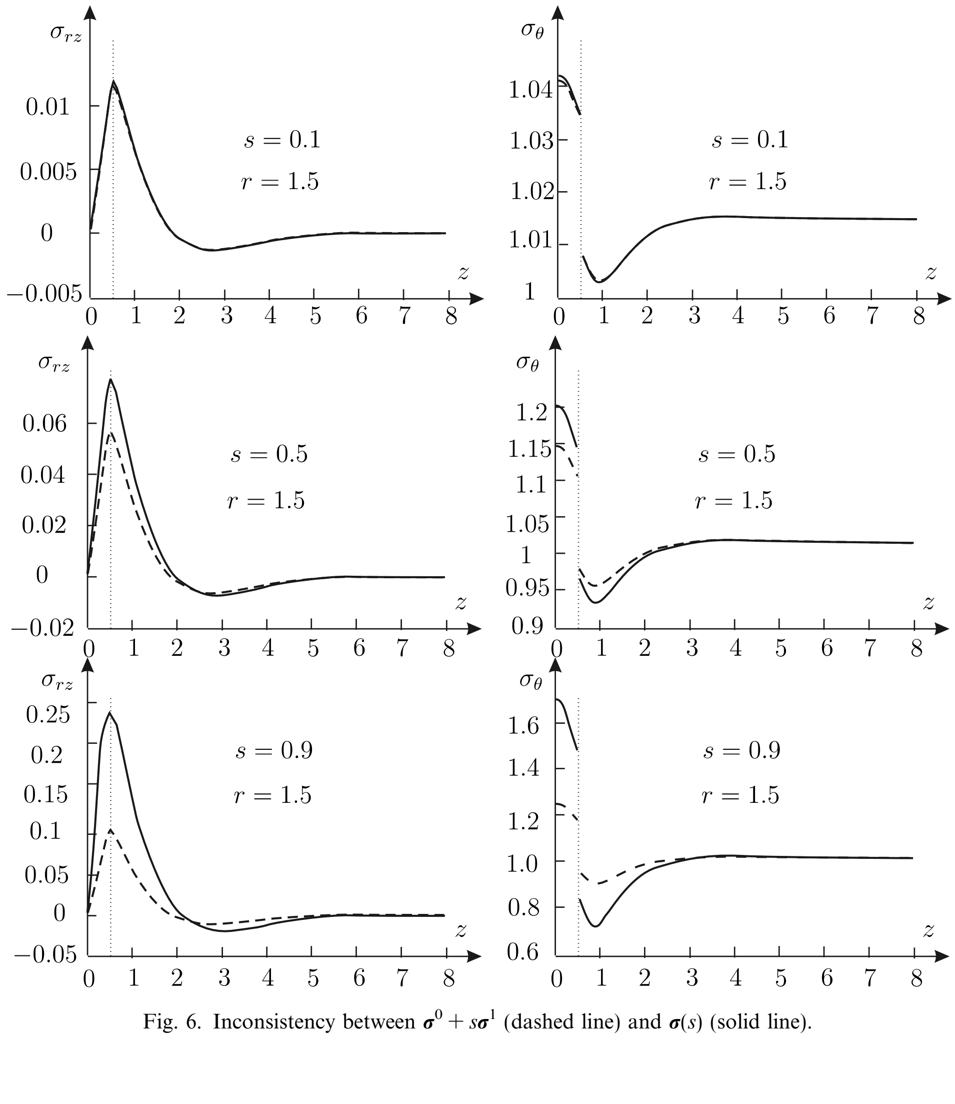

Fig. 6. Inconsistency between $\boldsymbol{\sigma}^0 + s\boldsymbol{\sigma}^1$ (dashed line) and $\boldsymbol{\sigma}(s)$ (solid line).

7. Discussion

The application of the perturbation method to the steady-state creep problem was investigated. High performance of this method in prediction of creep response was validated. The perturbation method allow one to reduce an initial nonlinear problem to the sequence of simpler ones.

This technique is especially attractive if the unperturbed solution is given in closed form as it was in this paper. Another example is the creep response of the thick-walled homogeneous pipe under plane stress conditions (Malinin, 1981). Such solution could be used for perturbation analysis of creep in open-ended pipes.

The error of the perturbation method becomes substantial when the creep properties differ from one another by one order of magnitude. Nevertheless we note that asymptotic expansion (15) gives a good simplified model of structure response. This model treats changes in parameter distribution as jumps of displacements in an auxiliary linear problem.

In that way, the solution for every complicated case of parameter distribution is represented as a combination of simple solutions.

Acknowledgement

A.V. Shutov is grateful for the support provided by the German Academic Exchange Service.

Appendix A

Assume $\varphi_1(r) = \psi_1(r) = \sin\left(\frac{r-r_i}{r_o-r_i}\pi\right)$, $r_i = 1$, $r_o = 2$. After integration in (38)–(40) we have the following values of constants:

$$a_1 \approx 41.134, \quad a_2 \approx 3.770, \quad a_3 \approx -0.237,$$

$$b_1 \approx 3.770, \quad b_2 \approx -0.237, \quad b_3 \approx 3.948, \quad b_4 \approx 0.780, \quad b_5 \approx 1.778,$$

$$k_1 \approx 3.602, \quad k_2 \approx -0.736, \quad k_3 \approx 1.777,$$

$$e_2 = 0, \quad e_3 \approx -1,777, \quad g_2 \approx 1,777.$$

The ODE (42) has four linearly independent solutions

$$\psi_2^{\mathrm{I}} = \mathrm{e}^{\mathrm{Re}(\lambda)z}\sin(\mathrm{Im}(\lambda)z), \quad \psi_2^{\mathrm{II}} = \mathrm{e}^{\mathrm{Re}(\lambda)z}\cos(\mathrm{Im}(\lambda)z),$$
$$\psi_2^{\mathrm{III}} = \mathrm{e}^{-\mathrm{Re}(\lambda)z}\sin(\mathrm{Im}(\lambda)z), \quad \psi_2^{\mathrm{IV}} = \mathrm{e}^{-\mathrm{Re}(\lambda)z}\cos(\mathrm{Im}(\lambda)z),$$

where λ is one of solutions of characteristic equation

$$k_3\lambda^4 + k_2\lambda^2 + k_1 = 0.$$

To be definite, we use

$$\lambda = 0.903 + 0.780i.$$

References

Altenbach, H., Kushnevsky, V., Naumenko, K., 2001. On the use of solid- and shell-type finite elements in creep-damage predictions of thin-walled structures. Arch. Appl. Mech. 71, 164–181.

Antman, S.S., 1995. Nonlinear Problems of Elasticity. Springer-Verlag, Berlin.

Browne, R.E.J., Cane, B., Parker, J.D., Walters, D., 1981. Creep failure analysis of butt welded tubes. In: Proceedings of the Conference on Creep and Fracture of Engineering Materials and Structures, Swansea, pp. 645–649.

Coleman, M.C., Parker, J.D., Walters, D., 1985. The behaviour of ferritic weldments in thick section CrMoV pipe at elevated temperatures. Int. J. Press. Vess. Piping 18, 277–310.

Hall, F.R., Hayhurst, D.R., 1991. Continuum damage mechanics modelling of high-temperature deformation and failure in a pipe weldment. Proc. R. Soc. Lond. A 443, 383–403.

Hayhurst, D.R., 2001. Computational continuum damage mechanics: its use in the prediction of creep in structures—past, present and future. In: IUTAM Symposium on Creep in structures. Kluwer Academic Publishers, pp. 175–188.

Hayhurst, D.R., Wong, M.T., Vakili-Tahami, F., 2001. The use of CDM analysis techniques in high temperature creep failure of welded structures. In: Proceedings of CREEP 7, Japan Society of Mechanical Engineering (Tsukuba, June 3–8, 2001), SA-10-6(106), pp. 519–526.

Hyde, T.H., Yehia, K., Sun, W., 1996. Observations on the creep of two-material structures. J. Strain Anal. 31 (6), 441–461.

Hyde, T.H., Yaghi, A., Proctor, M., 1998. Use of the reference stress method in estimating the life of pipe bends under creep conditions. Int. J. Press. Vess. Piping 75, 161–169.

Hyde, T.H., Sun, W., Williams, J.A., 1999. Prediction of creep failure life of internally pressurized thick walled CrMoV pipes. Int. J. Press. Vess. Piping 76, 925–933.

Hyde, T.H., Sun, W., Tang, A., Budden, P.J., 2000. An inductive procedure for determining the stresses in multimaterial components under steady state creep. J. Strain Anal. 35 (5), 347–358.

Hyde, T.H., Sun, W., Williams, J.A., 2003. Creep analysis of pressurized circumferential pipe weldments—A review. J. Strain Anal. 38 (1), 1–29.

Kachanov, L.M., 1986. Introduction to Continuum Damage Mechanics. Martinus Nijhoff Publishers, Dordrecht.

Kantorovich, L.V., Krylov, V.I., 1958. Approximate Methods of Higher Analysis. Interscience Publ., New York.

Leckie, F.A., Hayhurst, D.R., 1974. Creep rupture of structures. Proc. R. Soc. Lond. A 340.

Malinin, N.N., 1981. Creep Calculations of Structural Elements. Mashinostroenie, Moscow (in Russian).

Naumenko, K., Altenbach, H., 2005. A phenomenological model for anisotropic creep in a multi-pass weld metal. Arch. Appl. Mech. 74 (11–12), 808–819.

Nikitenko, A.F., Zaev, V.A., 1979. Design calculation of structural elements with vulnerability of the material in creep taken into account. Strength Mater. (Historical Archive) 11 (4), 354–360.

Odqvist, K.G., 1974. Mathematical Theory of Creep and Creep Rupture. Oxford University Press, Oxford.

Perrin, I.J., Hayhurst, D.R., 1999. Continuum damage mechanic analyses of type IV creep failure in ferritic steel crossweld specimens. Int. J. Press. Vess. Piping 76, 599–617.

Perrin, I.J., Hayhurst, D.R., Ainsworth, R.A., 2000. Approximate creep rupture lifetimes for butt welded ferritic steel pressurized pipes. Eur. J. Mech. A/Solids 19, 223–258.

Roche, R.L., Townley, C.H.A., Regis, V., Hubel, H., 1992. Structural analysis and available knowledge. In: Larson, L.H. (Ed.), High Temperature Structural Design. Mechanical Engineering Publications, London, pp. 161–180.

Washizu, K., 1982. Variational Methods in Elasticity and Plasticity. Pergamon, Oxford.